Dalton Transactions

Cite this: *Dalton Trans.*, 2012, **41**, 12888

www.rsc.org/dalton

PAPER

Cobalt complexes bearing scorpionate ligands: synthesis, characterization, cytotoxicity and DNA cleavage†‡

Telma F. S. Silva,[a] Luísa M. D. R. S. Martins,[a,b] M. Fátima C. Guedes da Silva,[a,c] Alexandra R. Fernandes,[a,c,d] Ana Silva,[c] Pedro M. Borralho,[e] Susana Santos,[a,c] Cecília M. P. Rodrigues[e] and Armando J. L. Pombeiro*[a]

Received 22nd August 2011, Accepted 29th August 2012
DOI: 10.1039/c2dt11577h

A number of novel, water-stable redox-active cobalt complexes of the C-functionalized tripodal ligands tris(pyrazolyl)methane $XC(pz)_3$ (X = $HOCH_2$, CH_2OCH_2Py or CH_2OSO_2Me) are reported along with their effects on DNA. The compounds were isolated as air-stable solids and fully characterized by IR and FIR spectroscopies, ESI-MS(+/−), cyclic voltammetry, controlled potential electrolysis, elemental analysis and, in a number of cases, also by single-crystal X-ray diffraction. They showed moderate cytotoxicity *in vitro* towards HCT116 colorectal carcinoma and HepG2 hepatocellular carcinoma human cancer cell lines. This viability loss is correlated with an increase of tumour cell lines apoptosis. Reactivity studies with biomolecules, such as reducing agents, H_2O_2, plasmid DNA and UV-visible titrations were also performed to provide tentative insights into the mode of action of the complexes. Incubation of Co(II) complexes with pDNA induced double strand breaks, without requiring the presence of any activator. This pDNA cleavage appears to be mediated by O-centred radical species.

Introduction

Scorpionates have become well-established ligands and their complexes have made important contributions in different areas, such as bioinorganic model ligand catalysis.[1,2] The popularity of scorpionate systems stems, in large part, from their flexibility that allows us to tune the electronic and steric features at a metal centre, *e.g.*, by substitution at the apical atom or at 3-, 4- or 5-position of the pyrazolyl rings. In particular, tris(pyrazolyl)-methane-type scorpionates $XC(Rpz)_3$ (pz = pyrazolyl; R = H or substituent at the pz ring; X = H or substituent), which are much less studied than the related tris(pyrazolyl)borates,[2] constitute an emerging field of research[2b,c] and provide a suitable entry for a fruitful coordination chemistry. Moreover, they can be fairly soluble in water, when bearing a suitable substituent, *e.g.* with a hydroxymethyl or a sulfonate group (X = $HOCH_2$, SO_3),[2a] what is of particular interest for catalytic applications in aqueous media, under environmentally friendly conditions, or for biological studies.

In pursuit of our recent work[3] on the coordination chemistry of $HC(Rpz)_3$ and derivatives,[3] we have now (i) selected some C-functionalized tris(pyrazolyl)methanes $XC(pz)_3$ (X = $HOCH_2$, CH_2OSO_2Me or CH_2OCH_2Py; Py = pyridyl), with a high hydrophilic nature, (ii) studied their coordination behaviour at a cobalt(II) centre; and (iv) tested the *in vitro* antitumor activity for the water-soluble compounds in two human cancer cell lines: HCT116 colorectal and HepG2 hepatocellular carcinomas.

Co coordination compounds can mimic some metalloenzymes and have been widely studied for the development of DNA-cleaving agents, enzyme inhibitors, hypoxic selective agents, nucleic acid probes, drug delivery devices, and positron emission tomography agents.[4–8] Cellular uptake of cobalt is carcinogenic at least in rodents due to genotoxicity by both radical-mediated mechanisms and direct cobalt interference with DNA repair probably by substituting zinc ions in zinc finger proteins.[4] The interest on cobalt complexes in experimental cancer therapy research results from their role as systemic anticancer agents and their ability to redox-dependent targeting the malignant tissue of solid tumours.[4–8] The former role was firstly attributed to the fact that vitamin B_{12} (cobalamin) is substituted together with folic acid in chemotherapy regimens involving antimetabolites to reduce unwanted side effects, and, secondly, to the fact that fast proliferating cells require higher amounts of vitamin B_{12} than normal ones. Cobalamin-conjugates with radioisotopes or

[a]*Centro de Química Estrutural, Complexo I, Instituto Superior Técnico, Technical University of Lisbon, Av. Rovisco Pais, 1049-001 Lisboa, Portugal. E-mail: pombeiro@ist.utl.pt*
[b]*Área Departamental de Engenharia Química, ISEL, R. Conselheiro Emídio Navarro, 1959-007 Lisboa, Portugal*
[c]*Universidade Lusófona de Humanidades e Tecnologias, ULHT Lisbon, Campo Grande 376, 1749-024 Lisboa, Portugal*
[d]*Departamento de Ciências da Vida, Faculdade de Ciências e Tecnologias, Universidade Nova de Lisboa, 2829-516 Caparica, Portugal*
[e]*Research Institute for Medicines and Pharmaceutical Sciences (iMed.UL), Faculty of Pharmacy, University of Lisbon, 1649-003 Lisboa, Portugal*

†Dedicated to Dr Christian Bruneau (Université de Rennes) on the occasion of his 60th anniversary.

‡Electronic supplementary information (ESI) available. CCDC 840090 (compound **1**), 840091 (compound **3**). For ESI and crystallographic data in CIF or other electronic format see DOI: 10.1039/c2dt11577h

cytotoxic compounds, *e.g.*, nitrosylcobalamin or a cisplatin–cobalamin, have been developed to achieve enhanced tumour accumulation *via* the respective receptor-mediated uptake system.[9,10] With regard to redox processes in the anticancer activity of cobalt complexes, two aspects have been of central interest: (i) activation of Co^{III} complexes in a hypoxic environment by reduction to Co^{II} and release of the ligand, and (ii) generation of reactive oxygen species (ROS) by a catalytic autooxidation process especially for Schiff base complexes. The reduction step of Co^{III} complexes might not only lead to the release of cytotoxic ligands but also to generation of ROS based on a catalytic autooxidation process.[11] As mentioned above, even Co^{II} ions themselves induce generation of ROS *in vivo* and *in vitro* by catalyzing the generation of hydroxyl radicals from H_2O_2 in a Fenton-like reaction.[7] Interestingly, it has been recently demonstrated that Co^{II} ions can replace Mg^{2+} in enzymatic physiological enzyme reactions, which strongly enhance DNA cleavage by topoisomerase IIα.[12]

In this regard, we report herein the potential role of the new water soluble scorpionate Co half-sandwich complexes obtained in this study as cytotoxic agents.

Experimental

General materials and procedures

Pyrazole, sulphur trioxide–trimethylamine complex (Aldrich), cobalt(II) chloride or nitrate, acetonitrile, tetrahydrofuran, diethyl ether, chloroform, methanol (Lab-Scan) were used as received from the supplier. $HC(pz)_3$,[13] $HOCH_2C(pz)_3$,[13] $Li[SO_3C(pz)_3]$,[14] $CH_3SO_2OCH_2C(pz)_3$ [15] and $PyCH_2OCH_2C(pz)_3$ [3b] were obtained according to published methods.

Infrared spectra (4000–400 cm^{-1}) were recorded on a BIO-RAD FTS 3000 MX in KBr pellets; wavenumbers are in cm^{-1}; abbreviations: vs, very strong; s, strong; m, medium; w, weak. Far infrared spectra Far-IR (400–200 cm^{-1}) were recorded on a Vertex 70 spectrophotometer in CsI pellets.

ESI^+/ESI^- mass spectra were obtained on a VARIAN 500-MS LC ion trap mass spectrometer (solvent: MeOH; flow: 20 μL min^{-1}; needle spray voltage: ±5 kV, capillarity voltage: ±100 V; nebulizer gas (N_2): 35 psi; drying gas (N_2): 10 psi; drying gas temperature (N_2): 350 °C). For the MS spectra description, M denotes the complex part of compounds **1–5**.

The C, H, N and S elemental analyses were carried out by the Microanalytical Service of the Instituto Superior Técnico.

The electrochemical experiments were performed on an EG&G PAR 273A potentiostat/galvanostat connected to a personal computer through a GPIB interface. Cyclic voltammograms (CV) were obtained in 0.2 M $[^nBu_4N][BF_4]$/NCMe or DMSO, at a platinum disc working electrode (d = 1 mm). Controlled-potential electrolyses (CPE) were carried out in electrolyte solutions with the abovementioned composition, in a three-electrode H-type cell. The compartments were separated by a sintered glass frit and equipped with platinum gauze working and counter electrodes. For both CV and CPE experiments, a Luggin capillary connected to a silver wire pseudo-reference electrode was used to control the working electrode potential. The CPE experiments were monitored regularly by cyclic voltammetry, thus assuring no significant potential drift occurred along the electrolyses. Ferrocene was used as an internal standard for the measurement of the oxidation potentials of the complexes; the redox potential values are quoted relative to the SCE by using as an internal reference the ferrocene/ferricinium couple ($[Fe(\eta^5\text{-}C_5H_5)_2]^{0/+}$; E = 0.42 V *vs.* SCE in NCMe or 0.44 V *vs.* SCE in DMSO).[16]

X-ray crystal structure determinations. The X-ray diffraction data of **1** and **3** were collected using a Bruker AXS-KAPPA APEX II diffractometer with graphite monochromated Mo-Kα radiation. Data were collected using omega scans of 0.5° per frame, and a full sphere of data was obtained. Cell parameters were retrieved using Bruker SMART software and refined using Bruker SAINT on all the observed reflections. Absorption corrections were applied using SADABS.[17a] Structures were solved by direct methods using the SHELXS-97 package and refined with SHELXL-97.[17b] Calculations were performed with the WinGX System-Version 1.80.03.[17c] All hydrogen atoms were inserted in calculated positions. CCDC numbers 840090 (compound **1**) and 840091 (compound **3**) contain the supplementary crystallographic data for this paper.

Synthesis and characterization of complexes

$[Co(OSO_3H)(OCH_3)(HOCH_3)\{HC(pz)_3\}]$ (1). To a solution of $CoCl_2$ (0.10 g, 0.80 mmol) in MeOH (10.0 mL) an equimolar amount of $Li[SO_3C(pz)_3]$ (0.23 g, 0.80 mmol) in MeOH (15.0 mL) was added, with stirring, under air. The resulting red solution was stirred overnight, then concentrated and, upon addition of Et_2O, a red solid precipitated. This was collected by filtration, washed with Et_2O and dried *in vacuo* (0.10 g, 29% yield). **1** is soluble in MeOH and DMSO ($S_{25\ °C} \approx 3.0$ mg mL^{-1}). Suitable crystals for X-ray analysis were obtained upon slow diffusion of Et_2O into a methanolic solution of the complex. IR (KBr pellet, cm^{-1}): 3529 [s, ν(O–H)], 1522 and 1412 [s, ν(C=C) and ν(N=C), $SO_3C(pz)_3^-$], 1206, 1102, 1054 [s, ν(S–O), $SO_3C(pz)_3^-$]. ESI^+-MS: m/z 400 ($[M - OCH_3]^+$), 384 ($[M - OCH_3 - O]^+$). Anal. calc. for $CoC_{12}H_{17}N_6O_6S$: C, 33.3; H, 4.0; N, 19.4; S, 7.4%. Found: C, 33.5; H, 3.9; N, 19.6; S, 7.2%.

$[Co\{HOCH_2C(pz)_3\}_2](NO_3)_2$ (2). To a solution of $HOCH_2C(pz)_3$ (200.0 mg, 0.81 mmol) in THF (10 mL) was added, with constant stirring, an equimolar amount of $Co(NO_3)_2{\cdot}6H_2O$ (235.3 mg, 0.809 mmol) in THF (20 mL), under continuous stirring for 3 h, at room temperature under air. The resulting pink solution was taken to dryness *in vacuo* and the pink solid thus obtained was washed with pentane (0.26 g, 48% yield). **2** is soluble in NCMe ($S_{25\ °C} \approx 4.4$ mg mL^{-1}). IR (KBr pellet, cm^{-1}): 3395 [m, ν(OH), $HOCH_2C(pz)_3$], 1629 and 1517 [m, ν(C=C), and ν(C=N), $HOCH_2C(pz)_3$], 1336 [s, ν(C–H), $HOCH_2C(pz)_3$]. ESI^+-MS: m/z 274 (M^{2+}). Anal. calc. for $CoC_{22}H_{24}N_{14}O_8$: C, 39.4; H, 3.6; N, 29.2%. Found: C, 39.1; H, 3.2; N, 29.1%.

$[Co\{HOCH_2C(pz)_3\}_2]{\cdot}[Co\{HOCH_2C(pz)_3\}(H_2O)_3]_2(Cl)_6{\cdot}6H_2O$ (3·6H$_2$O). To a solution of $HOCH_2C(pz)_3$ (98.7 mg, 0.40 mmol) in H_2O or MeOH (10 mL) was added, with constant stirring, an equimolar amount of $CoCl_2{\cdot}6H_2O$ (73.4 mg, 0.40 mmol) in H_2O or MeOH (10 mL), under continuous stirring

for 3 h under air, at room temperature. The resulting green solution was taken to dryness *in vacuo* and a green solid was thus obtained (0.098 g, 47% yield). **3** is soluble in water ($S_{25\ °C} \approx$ 5.0 mg mL^{-1}), MeOH and EtOH. Suitable crystals for X-ray analysis were obtained upon slow diffusion of Et_2O into a methanolic solution of the complex. IR (KBr pellet, cm^{-1}): 3382 [m, ν(OH), $HOCH_2C(pz)_3$], 1619 and 1518 [m, ν(C═C), and ν(C═N), $HOCH_2C(pz)_3$], 1336 [s, ν(C–H), $HOCH_2C(pz)_3$]. ESI^+-MS: *m/z* 274 ($[Co\{HOCH_2C(pz)_3\}_2]^{2+}$), 207 ($[Co\{HOCH_2C(pz)_3\}_2 - pz]^{2+}$). Anal. calc. for $Co_3C_{44}H_{72}N_{24}O_{16}Cl_6$: C, 33.5; H, 4.7; N, 20.8%. Found: C, 33.3; H, 4.3; N, 20.7%.

$[CoCl_2(H_2O)\{PyCH_2OCH_2C(pz)_3\}]$ (4). To a solution of $CoCl_2{\cdot}6H_2O$ (0.21 g, 0.90 mmol) in THF (20 mL) an equimolar amount of $PyCH_2OCH_2C(pz)_3$ (0.30 g, 0.90 mmol) in THF (10 mL) was added, with constant stirring, under air, resulting in a blue solution. A few minutes later, a blue solid precipitated. It was collected by filtration, washed with pentane and dried *in vacuo* (0.26 g, 60% yield). **4** is soluble in H_2O ($S_{25\ °C} \approx$ 2.2 mg mL^{-1}), MeOH and NCMe. IR (KBr pellet, cm^{-1}): 3406 and 1620 [s, $\nu(H_2O)$], 1561 and 1518 [s, ν(C═C) and ν(N═C), $PyCH_2OCH_2C(pz)_3$], 866, 760 and 653 [s, $PyCH_2OCH_2C(pz)_3$]. Far-IR (CsI pellet, cm^{-1}): 312 [m, ν(Co–Cl)]. ESI^+-MS: *m/z* 429 ($[M - H_2O - Cl]^+$), 362 ($[M - H_2O - Cl - pz]^+$). Anal. calc. for $CoC_{17}H_{19}N_7O_2Cl_2$: C, 42.3; H, 4.0; N, 20.2%. Found: C, 41.9; H, 4.1; N, 19.9%.

$[CoCl_2(H_2O)\{CH_3SO_2OCH_2C(pz)_3\}]$ (5). To a solution of cobalt chloride (0.10 g, 0.77 mmol) in MeOH (20 mL) an equimolar quantity of $H_3CSO_2OCH_2C(pz)_3$ (0.25 g, 0.77 mmol) in MeOH (30 mL) was added, with constant stirring. The resulting green solution was stirred overnight, then concentrated and, upon addition of Et_2O, a green solid precipitated. The solid was collected by filtration, washed with Et_2O and dried *in vacuo* (0.21 g, 58% yield). **5** is soluble in H_2O ($S_{25\ °C} \approx$ 2.0 mg mL^{-1}), MeOH and NCMe. IR (KBr pellet, cm^{-1}): 3430 and 1628 [s, $\nu(H_2O)$], 1521 and 1413 [s, ν(N═C), (N═N), $CH_3SO_2OCH_2C(pz)_3$], 1029 and 643 [s, ν(S═O), (C–S), $CH_3SO_2OCH_2C(pz)_3$]. Far-IR (CsI pellet, cm^{-1}): 300 and 290 [m, ν(Co–Cl)]. ESI^+-MS: *m/z* 417 ($[M - H_2O - Cl]^+$): C, 350 ($[M - H_2O - Cl - pz]^+$). Anal. calc. for $CoC_{12}H_{16}N_6O_4Cl_2S$: C, 30.7; H, 3.4; N, 17.8; S, 6.9%. Found: C, 31.0; H, 3.3; N, 18.1; S, 6.8%.

Assessment of the cytotoxicity of the water soluble compounds

Cell culture. HCT116 human colorectal carcinoma cells were grown in Dulbecco's modified Eagle's medium (DMEM) (Invitrogen Corp., Grand Island, NY, USA) supplemented with 10% fetal bovine serum and 1% antibiotic/antimycotic solution (Invitrogen Corp.) and maintained at 37 °C in a humidified atmosphere of 5% CO_2. HepG2 human hepatocellular carcinoma cells were grown under similar conditions, supplemented with 1% MEM non-essential amino acid (Invitrogen Corp.).

Compound exposure. Stock solutions of 0.1–4 mM were prepared in sterile double distilled water. For the dose–response curves, cells were plated at 5000 cells per well in 96-well plates. Media were removed 24 h after platting and replaced with fresh media containing: 0.1, 0.5, 1 and 2 mM complex **3**; 0.1, 0.5, 1, 2 and 4 mM complex **4**; and 0.25, 0.5, 1, 2 mM complex **5**; or water (vehicle control).

Viability assays. After 48 h of cell incubation in the presence or absence of each compound, cell viability was evaluated with a CellTiter 96® AQueous Non-Radioactive Cell Proliferation Assay (Promega, Madison, WI, USA), using 3-(4,5-dimethylthiazol-2-yl)-5-(3-carboxymethoxyphenyl)-2-(4-sulfophenyl)-2*H*-tetrazolium, inner salt (MTS). In brief, this is a homogeneous, colorimetric method for determining the number of viable cells in proliferation, cytotoxicity or chemosensitivity assays. The CellTiter 96® AQueous Assay is composed of solutions of MTS and an electron coupling reagent (phenazinemethosulfate, PMS). MTS is bioreduced by cells into a formazan product that is soluble in a tissue culture medium. The absorbance of the formazan product at 490 nm can be measured directly from 96-well assay plates without additional processing. The conversion of MTS into the aqueous soluble formazan product is accomplished by dehydrogenase enzymes found in metabolically active cells. The quantity of the formazan product was measured in a Bio-Rad microplate reader Model 680 (Bio-Rad, Hercules, CA, USA) at 490 nm, as absorbance is directly proportional to the number of viable cells in culture.

Assessment of apoptosis for the water soluble compounds

Hoechst 33258 labelling. HCT116 cells were grown in a DMEM culture medium (Invitrogen, Grand Island, NY, USA) supplemented with 10% fetal bovine serum (Invitrogen) and 1% antibiotic/antimycotic solution (Invitrogen), and maintained at 37 °C in a humidified atmosphere of 5% CO_2. Cells were plated at 7500 cells per mL and incubated for 48 h in a culture medium containing the studied compounds dissolved in distilled water, or without addition (control). Hoechst staining was used to detect apoptotic nuclei. The medium was removed, cells were washed with phosphate-buffered saline 1X (PBS) (Invitrogen), and fixed with 4% paraformaldehyde in PBS1X (Invitrogen) for 10 min in the dark. Cells were incubated with Hoechst dye 33258 (Sigma, Missouri, USA) at 5 μg mL^{-1} in PBS 1X (Invitrogen) for 10 min, washed with PBS 1X (Invitrogen) and mounted using 20 μL of PBS : glycerol (3 : 1; v/v) solution. Fluorescent nuclei were sort out according to the chromatin condensation degree and characteristics. Normal nuclei showed non-condensed chromatin uniformly distributed over the entire nucleus. Apoptotic nuclei showed condensate or fragmented chromatin. Some cells formed apoptotic bodies. Plates were photographed in an AXIO Scope (Carl Zeiss, Oberkochen, Germany), and three random microscopic fields per sample with *ca.* 50 nuclei were counted. Mean values were expressed as the percentage of apoptotic nuclei.

Statistical analysis

All data were expressed as mean ± SEM from at least three independent experiments. Statistical significance was evaluated using the Student's *t*-test; $p < 0.05$ was considered statistically significant.

Interaction between the water soluble compounds and plasmid DNA

The interactions between compounds and pBluescript II SK(+) (pBSKII) DNA (Agilent Technologies, California, USA) and pUC18 (2686 bp) (Fermentas, USA) were determined.

Plasmids were obtained from *E. coli* transformed cells, grown overnight (o.n.) in an LB liquid medium (Applichem, Darmstadt, Germany) with 100 μg mL^{-1} Ampicillin (Bioline, London, UK), at 37 °C with stirring. Plasmid extractions were performed using the Invisorb® Spin Plasmid Mini Two Kit (Invitek, Berlin, Germany) and DNA were quantified by spectrophotometry with NanoDrop 2000 (Thermo Scientific, Massachusetts, USA). Both plasmids contained over 95% of supercoiled DNA with a faint relaxed DNA band. The restriction enzymes *DraI* (three recognition sites of TTTAAA at positions 1565, 1584 and 2276 of pUC18) and *SmaI* (recognition site GGGCCC at position 436 of pUC18) were used for the digestion of the supercoiled DNA.

Compound–DNA interaction assays were performed in tubes containing 200 ng of plasmid DNA and tested compounds at different concentrations in the presence and in the absence of the activating agent H_2O_2 (200 μM). It was added Tris-HCl buffer (Merck) 5 mM, NaCl (Panreac) 50 mM, pH 7.0, for a final volume of 20 μL. A control sample was also prepared with plasmid DNA and buffer using the same method described above. A typical reaction mixture, containing supercoiled plasmid DNA, and complexes **3**, **4** and **5** in Tris-HCl buffer (Merck) 5 mM, NaCl (Panreac) 50 mM, pH 7.0, was incubated at 37 °C for 4 h (with or without additives, or without any external reductant). After the incubation period, the reactions were quenched by keeping the samples at −20 °C followed by addition of 4 μL of loading buffer (25 mM Tris-HCl, 25 mM EDTA (pH = 8.0), 50% glycerol, 0.1% of bromophenol blue). Samples were then loaded on a 0.8% agarose gel (p/v) (Agarose SeaKem®LE, Maine, USA) dissolved in TAE buffer 1× (4.84 g Tris-Base (Merck), EDTA (Riedel-de Haën) 0.5 M, 1.142 mL acetic acid (Panreac), pH 8.0). The electrophoresis was performed at 80 V as constant voltage for 2 h in 1× TAE buffer. The DNA was stained by immersing the agarose gel in an ethidium bromide solution (0.5 mg L^{-1} in distilled water) for 20 min, afterwards the gel was washed in distilled water for 10 min and the results were analyzed and photographed using a UVI TEC transilluminator (Cambridge, UK) coupled to a Kodak Alpha-DigiDoc camera (Alpha Innotech, California, USA), and using AlphEaseFC software (AlphaDigiDoc 1000, Alpha Innotech) for image acquisition.

UV-visible titrations

The interaction of the complexes with Calf Thymus (CT) DNA was studied by UV-visible spectroscopy between 230 and 700 nm. UV spectra were recorded for a constant complex concentration, in the absence and presence of CT DNA at crescent concentrations. All solutions were prepared in Tris-HCl 5 mM, NaCl 50 mM buffer (pH 7.0). CT DNA concentration in base pairs had been determined at 260 nm in a NanoDrop2000 spectrophotometer (ThermoScientific), using an extinction coefficient of 6600 M^{-1} cm^{-1}.

Results and discussion

Synthesis of complexes and spectroscopic characterization

The attempt to synthesise a cobalt complex bearing the hydrophilic anionic tris(pyrazolyl)methanesulfonate ligand, from the reaction of $Li[SO_3C(pz)_3]$ (pz = pyrazolyl) with cobalt(II) chloride (in stoichiometric amounts) in methanol, led to the formation of the tris(pyrazolyl)methane Co(II) complex $[Co(OSO_3H)(OCH_3)(HOCH_3)\{HC(pz)_3\}]$ (**1**) (reaction *a*, Scheme 1). Rupture of the $C(sp^3)$–S bond at $^{-}O_3S$–$C(pz)_3$ conceivably occurred by metal-promoted hydrolysis, leading to the parent $HC(pz)_3$ and hydrogenosulfate HSO_4^- that coordinate to the metal which, in the final complex, also bears methoxide and solvent methanol as ligands. The compounds with the neutral scorpionates $[Co\{HOCH_2C(pz)_3\}_2](NO_3)_2$ (**2**), $[Co\{HOCH_2C(pz)_3\}_2]\cdot[Co\{HOCH_2C(pz)_3\}(H_2O)_3]_2(Cl)_6\cdot 6H_2O$ (**3**·$6H_2O$), $[CoCl_2(H_2O)\{PyCH_2OCH_2C(pz)_3\}]$ (Py = pyridyl) (**4**) and $[CoCl_2(H_2O)\{CH_3SO_2OCH_2C(pz)_3\}]$ (**5**) were obtained by reactions of CoX_2 (X = Cl^- or NO_3^-) with the appropriate neutral C-functionalized tris(pyrazolyl)methane (reactions *b*–*e*, Scheme 1). They provide, to our knowledge,[2] the first examples of Co(II) complexes bearing such scorpionate ligands, *i.e.*, $HOCH_2C(pz)_3$, $PyCH_2OCH_2C(pz)_3$ and $CH_3SO_2OCH_2C(pz)_3$.

All the complexes are stable in air and **3**, **4** and **5** display fair solubilities in water ($S_{25\ °C}$ *ca.* 2–5 mg mL^{-1}), an important feature towards their application (see below) as tumour-inhibiting agents against human tumour cell lines.

The complexes were characterized by elemental analysis, IR spectroscopy, ESI-MS, cyclic voltammetry and controlled potential electrolysis and, for **1** and **3**, also by single-crystal X-ray diffraction analysis.

Their IR spectra display ν(C=C) and ν(C=N) bands of pyrazolyl or pyrazole groups at the normal[3] range of 1626–1510 cm^{-1}. **2** and **3** exhibit medium intensity bands in the 3395–3382 cm^{-1} range assigned to ν(OH) of the ligated $HOCH_2C(pz)_3$.[3d] For **4** and **5**, the medium intensity ν(Co–Cl) bands in the 312–275 cm^{-1} range confirm the presence of the chloride ligands. In **4**, $PyCH_2OCH_2C(pz)_3$ is coordinated *via* the three pyrazolyl rings, leaving uncoordinated the pyridyl group, a behaviour that is similar to that found at, *e.g.*, $[VOCl_2\{PyCH_2OCH_2C(pz)_3\}_2]$.[3b]

The ellipsoid plots of complexes **1** and **3** are depicted in Fig. 1 and 2. Crystallographic data and selected bonding parameters are given in Tables S1 and S2,‡ respectively. The geometry around the cobalt ions in both complexes is of octahedral type. Compound **1** (Fig. 1) is a half sandwich Co(II) compound which occurs as a hydrogen bonded molecular aggregate due to the strong interaction between the HSO_3 moiety of one molecule and an O-methoxy atom from another [*d*(D···A) O5–H5A···O1 2.663(4) Å, ∠(DHA) 162.4 °]. In the asymmetric unit of **3** (Fig. 2) half a discorpionate Co(II) complex (the metal is located in an inversion centre) and a monoscorpionate tri-aqua Co(II) unit were found, together with three chloride anions and three crystallization water molecules.

The crystal packing diagram of **3** (Fig. S1a‡) shows that the crystallization water molecules and the chloride counterions form cyclic $\{(H_2O)_6Cl_4\}^{4-}$ clusters which are further hydrogen bonded to two other chloride anions, the set occupying the free

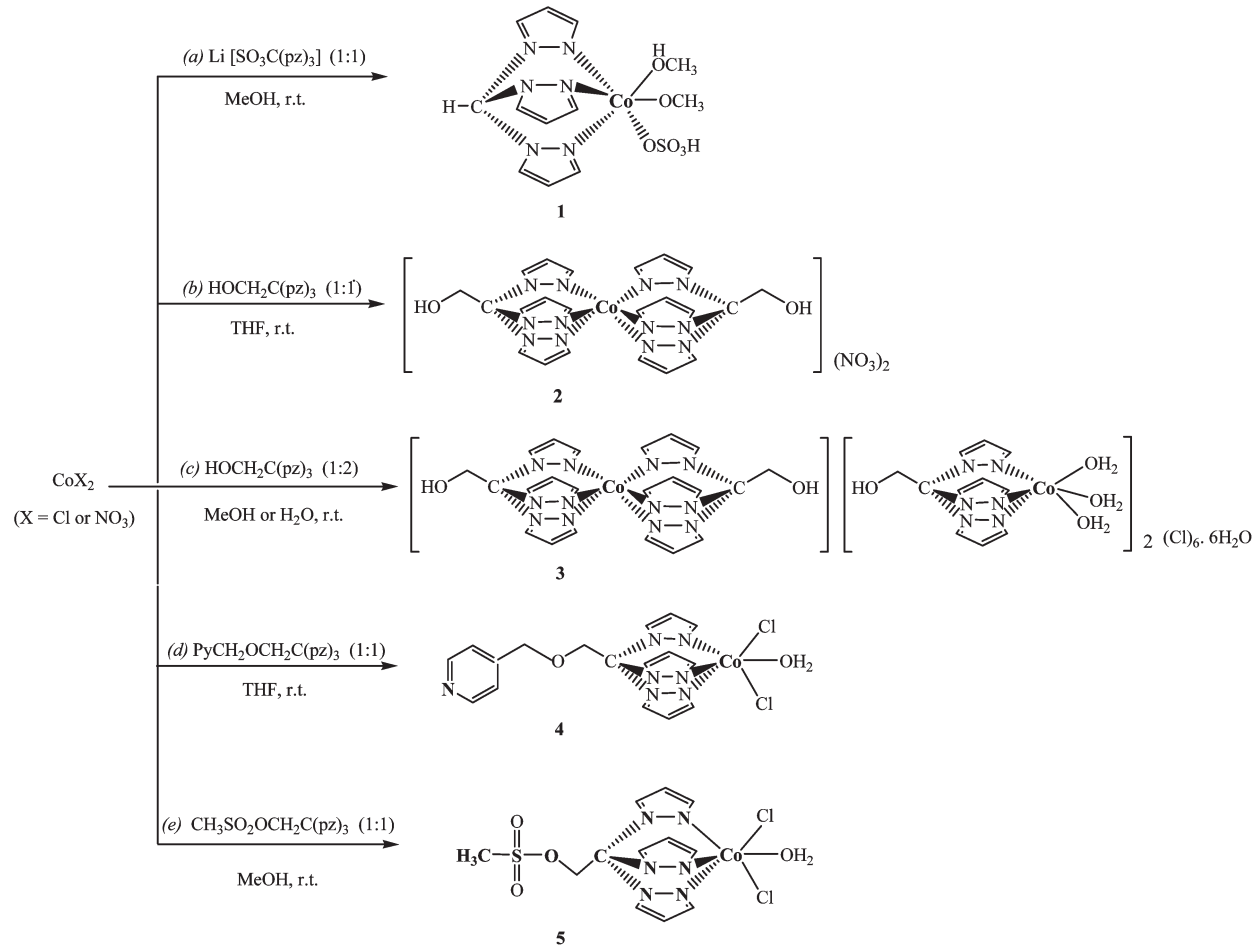

Scheme 1

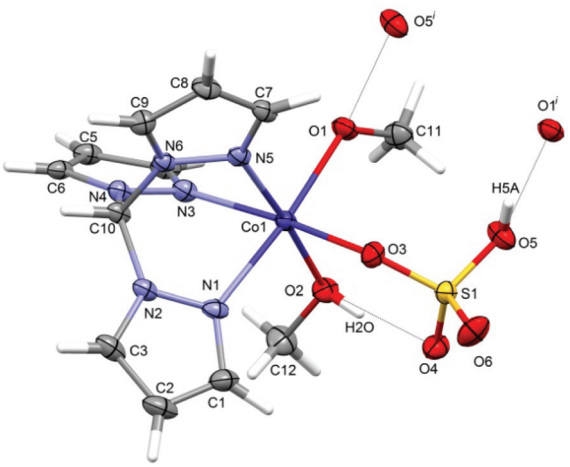

Fig. 1 Crystal structure of complex **1** with an atomic numbering scheme (ellipsoid probability level of 50%) showing in dotted lines the intra- and intermolecular H bond interactions. Distances *d*(D···A) and angles ∠(D–H···A) O2–H2O···O4 [2.584(4) 157(5)], O5–H5A···O1[i] [2.663(4) 162.4]. Symmetry operation to generate equivalent atoms: (i) $-x+1, -y, -z+1$.

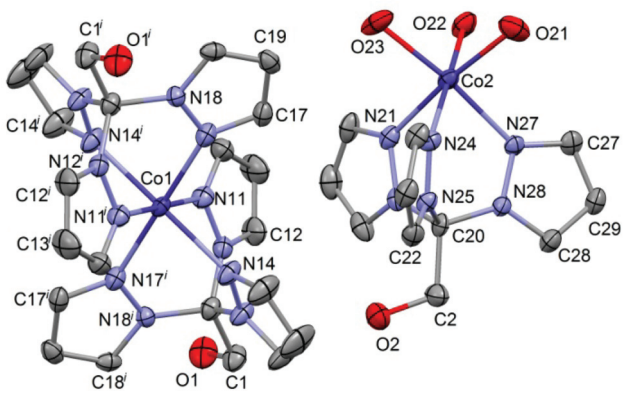

Fig. 2 Crystal structure of complex **3** with an atomic numbering scheme (ellipsoid probability level of 50%). The hydrogen atoms, the water molecules and the chloride counter-ions were omitted for clarity. Symmetry operations to generate equivalent atoms: (i) $1-x, 2-y, -z$.

space between the metal–organic entities. As found in other water–chloride networks[18] and extended assemblies,[19] the incorporation of our $\{(H_2O)_4(Cl)_4(Cl)_2\}^{6-}$ units in **3** is strongly supported by intermolecular interactions (Fig. S1b and Table S3 in ESI‡ file).

The cyclic $\{(H_2O)_4(Cl)_4(Cl)_2\}^{6-}$ fragment is constructed by means of two O–H···O interactions with O···O distances of 2.801 Å and ten O–H···Cl hydrogen bonds (Fig. 3b) with O···Cl

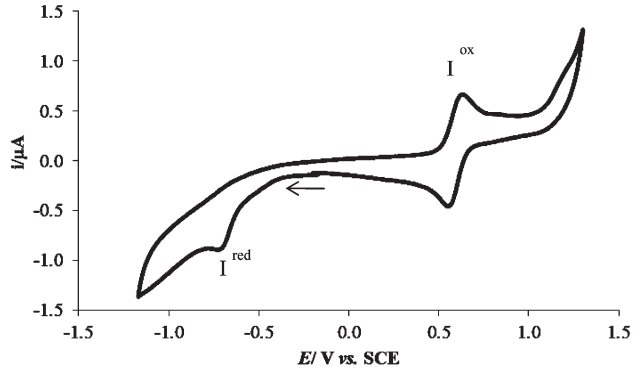

Fig. 3 Cyclic voltammogram of **2**, at a Pt disc electrode, in a 0.20 M [^{n}Bu$_4$N][BF$_4$]/NCMe solution. Complex concentration: 1.5 mM.

separations in the 3.090–3.384 Å range (Table S1‡). Both the O···O and the average of O···Cl (~3.08 Å) separations are comparable to those found in liquid water (*i.e.* 2.85 Å)[20] and various types of H_2O[21,22] hybrid H_2O–Cl[23] clusters.

Electrochemical studies

The redox properties of the complexes were studied by cyclic voltammetry (CV) and controlled potential electrolysis. By CV at a Pt disc electrode, in 0.2 M [^{n}Bu$_4$N][BF$_4$]/NCMe (or DMSO for **1**) solutions, each of the complexes exhibits a single-electron irreversible reduction wave (I^{red}) in the range of −0.40 to −0.68 V *vs.* SCE assigned to the $Co^{II} \rightarrow Co^{I}$ reduction process and a single-electron irreversible (for **1**, **4** or **5**) or reversible (for **2** and **3**) oxidation wave (I^{ox}) which concerns the $Co^{II/III}$ oxidation, at the oxidation potential values ($^{I}E^{ox}_{p/2}$ or $^{I}E^{ox}_{1/2}$ in the range of 0.58–1.28 V *vs.* SCE) (Table 1, and Fig. 3 for **2**). Moreover, compound **3**, with two Co centres, displays two irreversible oxidation and reduction waves, one for each Co^{II} site. For **3**, the first reduction and the first oxidation waves are assigned to the full-sandwich Co moiety $[Co\{HOCH_2C(pz)_3\}_2]^{2+}$ since they occur at redox potential values ($^{I}E^{red}_{p/2}$ = −0.67 V, $^{I}E^{ox}_{1/2}$ = 0.60 V *vs.* SCE) that are identical to those of **2**. Moreover, in the case of **3**, with Cl^- as the counterion, an irreversible oxidation wave is observed at E^{ox}_p = 1.28 V *vs.* SCE, being assigned to the oxidation of Cl^-.

Viability assays and Hoechst staining

Antiproliferative activities of the water soluble compounds $[Co\{HOCH_2C(pz)_3\}_2]\cdot[Co\{HOCH_2C(pz)_3\}(H_2O)_3]_2(Cl)_6\cdot 6H_2O$ (**3**·6H$_2$O), $[CoCl_2(H_2O)\{PyCH_2OCH_2C(pz)_3\}]$ (**4**) and $[CoCl_2(H_2O)\{CH_3SO_2OCH_2C(pz)_3\}]$ (**5**) were evaluated *in vitro* by the MTS metabolism assay, in HCT116 colorectal carcinoma and HepG2 hepatocellular carcinoma human cancer cell lines (Fig. 4).

Our results demonstrate that a 2 mM concentration of complexes **3**, **4** or **5** significantly decreases HCT116 cell viability to 23, 30 or 22%, respectively, compared to control cells ($p < 0.01$) (Fig. 4). In addition, a similar concentration of these complexes also significantly decreases HepG2 cell viability to 22, 23 and 27%, respectively ($p < 0.01$) (Fig. 4). Complex **3** is the most effective one in reducing cell viability. Despite the fact that these compounds present higher IC_{50} values for HCT116 (280, 418 and 658 μM for complexes **3**, **4** and **5**, respectively) and HepG2 (130, 391 and 626 μM for complexes **3**, **4** and **5**, respectively) tumour cells than the common antitumor drugs cisplatin (4.14 μM)[24] and doxorubicin (1.4 μM),[25] their water solubility may allow direct parenteral administration.

Table 1 Cyclic voltammetric data[a] for compounds **1–5**

Compound	$^{I}E^{red}_{p/2}$	$^{II}E^{red}_{p/2}$	$^{I}E^{ox}_{p/2}$($^{I}E^{ox}_{1/2}$)	$^{II}E^{ox}_{p/2}$
1[b]	−0.40	—	1.03	—
2	−0.68	—	(0.58)	—
3[c]	−0.67	−1.21	(0.60)	1.20
4	−0.60	—	1.28	—
5	−0.64	—	1.10	—

[a] Values in $V \pm 0.02$ relative to SCE; scan rate of 200 mV s^{-1}, in NCMe, unless stated otherwise. [b] In DMSO. [c] $E^{ox}_p(Cl^-)$ at 1.28 V.

The bioactivity does not seem to correlate with the redox potential of the complexes (see above), what is not unexpected since the complexes already bear the metal with the known[26] active oxidation state II. Their anti-tumour activity does not require, *e.g.* their prior reduction from Co(III) to Co(II), in contrast to other reported cases.[26]

In order to get an insight into the mechanism of cytotoxic action of our complexes in tumour cells, Hoechst nuclei staining of HCT116 cell lines in the absence (negative control) or in the presence of different concentrations of complexes **3**, **4** or **5** and doxorubicin (as a positive control of apoptotic nuclei) was assessed (Fig. 5 and results not shown).

Hoechst 33342 (2′-[4-ethoxyphenyl]-5-[4-methyl-1-piperazinyl]-2,5′-bi-1*H*-benzimidazole trihydrochloride trihydrate) is a cell-permeable DNA stain that is excited by ultraviolet light and emits blue fluorescence at 460 to 490 nm.[27] It binds preferentially to adenine–thymine (A–T) regions of DNA and it can detect gradations of nuclear damage and apoptosis. Normal nuclei show non-condensed chromatin uniformly distributed over the entire nucleus, whereas apoptotic nuclei show condensate or fragmented chromatin. Some cells form apoptotic bodies.[27]

The results shown in Fig. 5 correlate with the above viability results in Fig. 4. Indeed, there is clearly a marked decrease in cell viability in the presence of complex **3** and this decreased viability can be correlated with an increased cell death by apoptosis (as a dose dependent mechanism).

DNA is generally the primary intracellular target of anticancer drugs, and their interactions can cause damage in cancer cells, block their division and result in cell death.[28–30] In this regard, we also tested the ability of complexes **3**, **4** and **5** to interact with plasmid DNA (pDNA) in the absence of H_2O_2 by incubating pDNA with increasing concentrations of the tested compounds for 24 h and subjecting these mixtures to agarose gel electrophoresis (Fig. 6).

Our complexes can induce pDNA strand breaks for all the tested concentrations verifying a dose dependent response in the FI–Fc transition for complexes **4** and **5** (Fig. 6, lanes 8–11 and 12–15, respectively). Regarding complex **3**, no differences between the three isoforms were detected for all the tested

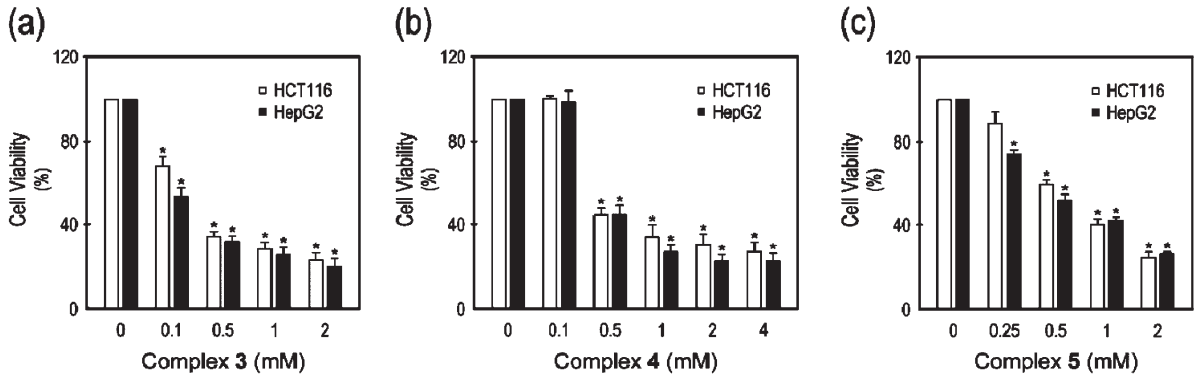

Fig. 4 Effect of complexes **3**, **4** and **5** exposures on HCT116 and HepG2 cell viability. Cells were exposed to: (a) 0.1–2 mM complex **3**; (b) 0.1–4 mM complex **4**; (c) 0.25–2 mM complex **5**; or water (vehicle control, 0 mM of complex) for 48 h. The results are expressed as mean ± SEM fold-change compared to controls from at least three independent experiments. The symbol * in the figure means that the results are statistically significant with a $p < 0.01$ (as compared to control for each compound and cell line).

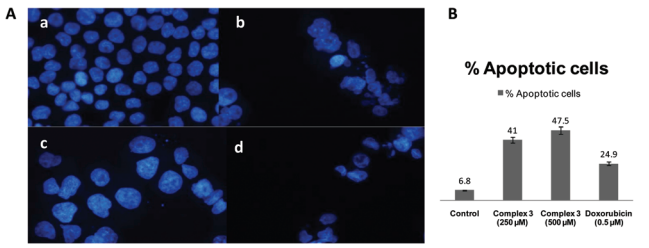

Fig. 5 A. Staining of HCT116 cell lines with Hoechst for the detection of apoptotic nuclei. Cells were grown in a DMEM culture medium supplemented with 10% fetal bovine serum in the absence (a), and the presence of 0.5 μM Doxorubicin (b), 250 μM complex **3** (c) and 500 μM complex **3** (d). Plates were photographed in an AXIO Scope (Carl Zeiss, Oberkochen, Germany). B. Mean values expressed as the percentage of apoptotic nuclei. Three random microscopic fields per sample with circa 50 nuclei were counted. Error bars represent standard deviations from the medium value of three independent experiments.

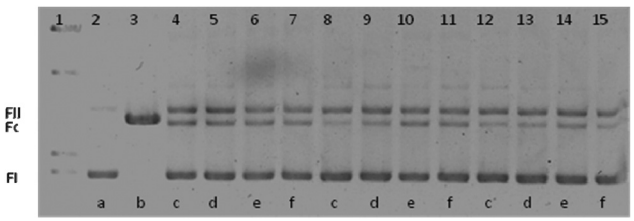

Fig. 6 Agarose gel electrophoresis (0.8% (w/v)) concerning the incubation of complexes **3**, **4** and **5** with pBSKII plasmidic DNA (pDNA) at pH = 7.0 and 37 °C for 24 h in the absence of H_2O_2. Lane 1: Molecular ladder λDNA/HindIII; lane 2: pBSKII (control); lane 3: linearized pBSKII; lanes 4–15: pBSKII DNA incubated in the presence of increasing concentrations [(c) 50 μM; (d) 100 μM; (e) 250 μM; and (f) 500 μM] of complexes **3** (lanes 4–7), **4** (lanes 8–11) or **5** (lanes 12–15). FI – supercoiled isoform of DNA; Fc – linear isoform of DNA (double strand breaks); FII – relaxed (nicked) isoform of DNA.

concentrations (Fig. 6, lanes 4–7) most probably due to compound saturation. Nevertheless, we can also observe the increase in the Fc isoform compared with control pDNA (Fig. 6 and 7). These results can only be explained by the capacity of compounds **3**, **4** and **5** to induce DNA breaks in the double helix. In the case of single strand cleavage, firstly an increase of FII would occur, resulting from a single cut of FI, and secondly this isoform (FII) would be converted into Fc as a result of cleavage nearby the first cleavage site.

It is known[26,31–34] that when redox-active metal complexes interact with DNA in the presence of dioxygen or a redox agent, reactive oxygen species can be generated, leading to strong DNA damage. In order to get an insight into the nature of this pDNA cleavage, we studied the effects of radical scavengers, ascorbic acid and H_2O_2. By performing the incubation of pDNA with complex **3** in the presence of the common hydroxyl radical scavenger DMSO, we observed a decrease in DNA cleavage (Fig. 7, lane 5 *vs.* lane 6, and Fig. S4,‡ lane 7 *vs.* lanes 5 and 6) supporting[31] the involvement of such a radical, namely *via* a Fenton type process. The presence of ascorbic acid seems to potentiate pDNA cleavage (Fig. 8, lanes 13–15), mainly for complex **4** where the FI isoform is no longer observed (lane 14). This is consistent with the reported pDNA cleavage by copper complexes in the presence of ascorbic acid,[35] and by the ascorbate–Cu(II) system,[36] and with the known[37] hydroxyl radical formation upon reaction of Cu(II) with ascorbic acid.

The incubation of pDNA with complex **3** in the presence of H_2O_2, a known hydroxyl radical source, seems to reduce the amount of the FI isoform, with a simultaneous increase in the FII isoform (Fig. 7, lane 9 *vs.* lane 6). Nevertheless, the presence of H_2O_2 does not appear to increase the amount of pDNA double strand cleavage observed with complex **3** alone (isoform Fc in Fig. 7, lane 9 *vs.* lane 6), suggesting that the process can also proceed *via* another radical. In this regard, it is noteworthy that radical metal-peroxo species Co(III)OO$^{\cdot}$ are known[38] to be formed upon reaction of a Co(II) complex with dioxygen. The abovementioned promotion of the Fc isoform by the presence of ascorbic acid is consistent with a reduction of Co(III) back to Co(II) by that acid making the system catalytic, both in the presence (isoform Fc in Fig. 7, lane 13 *vs.* lane 9) or absence of H_2O_2 (Fig. 7, lane 12 *vs.* lane 6). The cleavage activity of the complexes was not inhibited by the presence of sodium azide and L-histidine, suggesting that singlet oxygen is not involved, in contrast to the reported[42] behaviour of some cobalt(II) picolinate complexes.

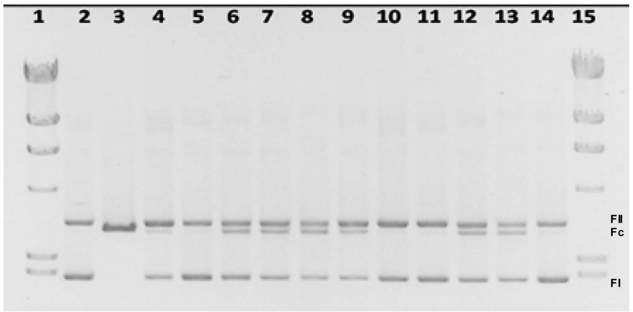

Fig. 7 Agarose gel electrophoresis (0.8% (w/v)) concerning the interaction between complex **3** (50 μM), **4** (100 μM) and **5** (100 μM) and pBSKII plasmidic DNA (pDNA) in the presence or absence of H_2O_2 (200 μM) and reductants. Lane 1 – Molecular ladder λDNA/HindIII; lane 2 – pBSKII (control); lane 3 – linearized pBSKII; lane 4 – pBSKII DNA incubated in the presence of H_2O_2 (200 μM); lane 5 – pBSKII DNA incubated in the presence of complex **3** and DMSO (2%); lane 6 – pBSKII DNA incubated in the presence of complex **3**; lane 7 – pBSKII DNA incubated in the presence of complex **4**; lane 8 – pBSKII DNA incubated in the presence of complex **5**; lane 9 – pBSKII DNA incubated in the presence of complex **3** and H_2O_2; lane 10 – pBSKII DNA incubated in the presence of ascorbic acid (50 μM); lane 11 – pBSKII DNA incubated in the presence of ascorbic acid (50 μM) and H_2O_2; lane 12 – pBSKII DNA incubated in the presence of complex **3** and ascorbic acid (50 μM); lane 13 – pBSKII DNA incubated in the presence of complex **3**, H_2O_2 and ascorbic acid (50 μM); lane 14 – pBSKII (control); lane 15 – Molecular ladder λDNA/HindIII. FI – supercoiled isoform of DNA; Fc – linear isoform of DNA (double strand breaks); FII – relaxed (nicked) isoform of DNA.

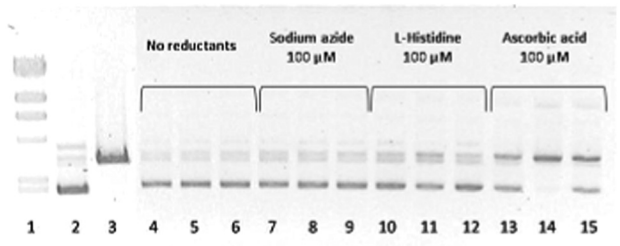

Fig. 8 Agarose gel electrophoresis (0.8% (w/v)) concerning the interaction between complex **3** (250 μM), **4** (250 μM) or **5** (250 μM) and pBSKII plasmidic DNA (pDNA) in the presence of H_2O_2 (200 μM). Lane 1 – Molecular ladder λDNA/HindIII; lane 2 – pBSKII (control); lane 3 – linearized pBSKII; lanes 4–6 – pBSKII DNA incubated in the presence of H_2O_2 and complexes **3**, **4** or **5**, respectively, without reductants; lanes 7–9 – pBSKII DNA incubated in the presence of H_2O_2 and complexes **3**, **4** or **5**, respectively, with sodium azide; lanes 10–12 – pBSKII DNA incubated in the presence of H_2O_2 and complexes **3**, **4** or **5**, respectively, with L-histidine; lanes 13–15 – pBSKII DNA incubated in the presence of H_2O_2 and complexes **3**, **4** or **5**, respectively, with ascorbic acid.

Despite the fact that several authors and also the IARC 2006 evaluation report have demonstrated that high doses of cobalt salts have a mutagenic potential *in vitro* and *in vivo*,[39–41] the incubation of pDNA with 50 μM of $CoCl_2$ and with the same concentration of complex **3** did not induce pDNA cleavage (Fig. S2,‡ lanes 4 and 2, respectively).

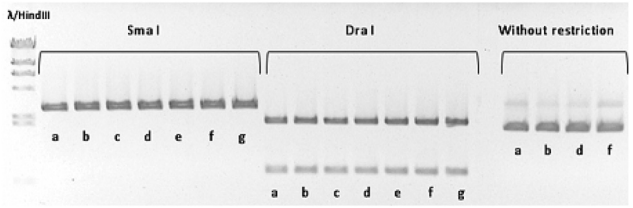

Fig. 9 Electrophoresis of the plasmid DNA pUC18 digested with the enzymes *SmaI* and *DraI* and without restriction enzymes: (a) complex **3** with $r = 0.3$; (b) complex **3** with $r = 0.1$; (c) complex **4** with $r = 0.3$; (d) complex **4** with $r = 0.1$; (e) complex **5** with $r = 0.3$; (f) complex **5** with $r = 0.1$; (g) pDNA (control). r = [complex]/[DNA].

DNA interaction studies

In order to understand if there was some specific interaction between any of the complexes **3**, **4** or **5** and the pDNA, digestion of pUC18 with the restriction enzymes *SmaI* and *DraI* which recognizes the base sequences –CCCGGG–, and –TTTAAA–, respectively, was performed (Fig. 9).

The analysis of the DNA samples showed no inhibition of the restriction enzyme *SmaI* by the presence of any of the complexes **3**, **4** or **5**, since we were only able to observe the presence of the linear form of pUC18 plasmid. Regarding *DraI* restriction, we were able to obtain two fragments of 1954 bp and 692 bp (the smaller fragment of 19 bp cannot be seen on this gel) which again indicates no interference of any of the complexes on the enzyme activity.

The absence of interaction between the cobalt complexes and CT DNA was also confirmed by spectroscopic studies through the incubation of complexes **3**, **4** or **5** with increasing concentrations of CT DNA. No hypochromic effect was observed under those conditions for all the complexes. For complex **4**, however, we observe (Fig. S3‡) a hyperchromic effect upon addition of CT-DNA which may indicate duplex DNA denaturation in the presence of such an elevated concentration of the complex.

Conclusions

We were able to prepare (i) the first tris(pyrazolyl)methane Co^{II} complex (**1**) upon the unusual $C(sp^3)$–SO_3 bond rupture at the sulfonate functionalized scorpionate and (ii) the first Co^{II} complexes (**2–5**) bearing the C-functionalized scorpionate ligands $HOCH_2C(pz)_3$, $PyCH_2OCH_2C(pz)_3$ and $CH_3SO_2OCH_2C(pz)_3$. The study thus contributed towards the development of the still little explored coordination chemistry of such types of scorpionate ligands.

The water soluble complexes **3**, **4** and **5** exhibit *in vitro* antiproliferative activities, although lower than that of cisplatin.[24] Nevertheless, we were able to correlate the viability loss of HCT116 tumour cell lines with an increase of apoptotic nuclei. *In vitro* DNA cleavage studies showed that, in the absence of an activator agent, Co(II)–scorpionate complexes induce pDNA double strand breaks, in a concentration dependent pattern, for complexes **4** and **5**. For complex **3**, the lower concentration tested in this work (50 μM) was already in the saturation level of induced double strand breaks. The pDNA cleavage appears to be mediated by O-centred radical species, namely the hydroxyl

radical, which, however, could not be unambiguously established. The presence of ascorbic acid seems to potentiate more rapidly the shift from isoform FI to Fc.

Despite the observed pDNA cleavage, we were not able to demonstrate direct interaction between the complexes and CT-DNA. Results from *in vitro* pDNA cleavage studies and from DNA binding experiments, from other groups, with cobalt complexes, although with different ligands, showed their ability to induce single strand cleavage and to have a moderate/strong affinity for CT-DNA.[31,42,43] As far as we know, our work provides the first observed double strand pDNA cleavage promoted by cobalt complexes bearing scorpionate ligands. On account of these initial results, further exploration of their mechanism and mode of action towards the biological targets in tumour cell lines will be addressed in order to understand namely if they may play an important role as specific and selective agents to cancer cells, while sparing healthy cells.

Moreover, the hydrophilicity of such complexes also encourages their potential use as catalyst precursors in an aqueous medium, namely for oxidations, what will also be investigated in our laboratory, in pursuit of our ongoing project in this field.[44]

Acknowledgements

This work has been partially supported by the Fundação para a Ciência e a Tecnologia (FCT), Portugal, and its "Strategic programme" PEst-OE/QUI/UI0100/2011. TFSS and PMB are grateful to FCT for PhD (SFRH/BD/48087/2008) and postdoctoral (SFRH/BPD/65212/2009) fellowships, respectively. The authors gratefully acknowledge Dr Maria Cândida Vaz (IST) for the direction of the elemental analysis service, the Portuguese NMR Network (IST-UTL Centre) for providing access to the NMR facility, the Portuguese MS Network (IST Node) (Dr Conceição Oliveira) for the ESI measurements, and Kelly Veiga for Hoechst staining assays.

References

1 (*a*) S. Trofimenko, *Scorpionates, The Coordination Chemistry of Polypyrazolylborate Ligands*, Imperial College Press, London, 1999; (*b*) C. Pettinari, *Scorpionates II: Chelating Borate Ligands*, Imperial College Press, London, 2008; (*c*) D. L. Reger and T. C. Grattan, *Synthesis*, 2003, 350–356; (*d*) R. V. Bernhardt and G. A. Lawrence, in *Comprehensive Coordination Chemistry II*, ed. J. A. McCleverty and T. J. Meyer, Elsevier, Oxford, 2004, vol. 6, ch 6; (*e*) B. Kräutler, in *Encyclopedia of Inorganic Chemistry*, ed. R. B. King, Wiley, 2nd edn, 2005, vol. 2.

2 (*a*) C. Pettinari and C. Santini, Polypyrazolylborate and scorpionate ligands, in *Comprehensive Coordination Chemistry II: From Biology to Nanotechnology*, ed. J. A. McCleverty and T. J. Meyer, Elsevier, Pergamon (APS), Amsterdam, 2003, vol. 1, pp. 159–210; (*b*) C. Pettinari and R. Pettinari, *Coord. Chem. Rev.*, 2005, **249**, 525; (*c*) H. R. Bigmore, C. S. Lawrence, P. Mountford and C. S. Tredget, *Dalton Trans.*, 2005, 635.

3 (*a*) T. F. S. Silva, M. F. C. Guedes da Silva, G. S. Mishra, L. M. D. R. S. Martins and A. J. L. Pombeiro, *J. Organomet. Chem.*, 2011, **696**, 1310; (*b*) R. Wanke, M. F. C. Guedes da Silva, S. Lancianesi, T. F. S. Silva, L. M. D. R. S. Martins, C. Pettinari and A. J. L. Pombeiro, *Inorg. Chem.*, 2010, **49**, 7941; (*c*) T. F. S. Silva, K. V. Luzyanin, M. V. Kirilova, M. F. C. Guedes da Silva, L. M. D. R. S. Martins and A. J. L. Pombeiro, *Adv. Synth. Catal.*, 2010, **352**, 171; (*d*) T. F. S. Silva, G. S. Mishra, M. F. C. Guedes da Silva, R. Wanke, L. M. D. R. S. Martins and A. J. L. Pombeiro, *Dalton Trans.*, 2009, 9207; (*e*) G. S. Mishra, T. F. S. Silva, L. M. D. R. S. Martins and A. J. L. Pombeiro, *Pure Appl. Chem.*, 2009, **81**, 1217; (*f*) T. F. S. Silva, E. C. B. Alegria, L. M. D. R. S. Martins and A. J. L. Pombeiro, *Adv. Synth. Catal.*, 2008, **350**, 706; (*g*) T. F. S. Silva, L. M. D. R. S. Martins, M. F. C. Guedes da Silva and A. J. L. Pombeiro, *Acta Crystallogr., Sect. E: Struct. Rep. Online*, 2007, **63**, m1979.

4 H. Chao and L.-N. Hi, in *Metallotherapeutic Drugs and Metal-based Diagnostic Agents: the use of Metals in Medicine*, ed. M. Gielen and E. R. T. Tiekink, John Wiley & Sons, England, 2005, ch. 11, pp. 201–218.

5 U. Jungwirth, C. R. Kowol, B. K. Keppler, C. G. Hartinger, W. Berger and P. Heffeter, *Antioxid Redox Signaling*, 2011, **15**, 1085.

6 M. E. Vol'pin, I. Levitin and S. P. Osinsky, *Met. Ions Biol. Syst.*, 1999, **36**, 485.

7 D. Beyersmann and A. Hartwig, *Arch. Toxicol.*, 2008, **82**, 493.

8 E. Kopera, T. Schwerdtle, A. Hartwig and W. Bal, *Chem. Res. Toxicol.*, 2004, **17**, 1452.

9 Y. Gupta, D. V. Kohli and S. K. Jain, *Crit. Rev. Ther. Drug Carrier Syst.*, 2008, **25**, 347.

10 P. Ruiz-Sanchez, C. Konig, S. Ferrari and R. Alberto, *J. Biol. Inorg. Chem.*, 2011, **16**, 33.

11 S. Osinsky, I. Levitin, L. Bubnovskaya, A. Sigan, I. Ganusevich, A. Kovelskaya, N. Valkovskaya, L. Campanella and P. Wardman, *Exp. Oncol.*, 2004, **26**, 140.

12 E. L. Baldwin, J. A. Byl and N. Osheroff, *Biochemistry*, 2004, **43**, 728.

13 D. L. Reger, T. C. Grattan, K. J. Brown, C. A. Little, J. J. S. Lamba, A. L. Rheingold and R. D. Sommer, *J. Organomet. Chem.*, 2000, **607**, 120.

14 W. Kläui, M. Berghahn, G. Rheinwald and H. Lang, *Angew. Chem., Int. Ed.*, 2000, **39**, 2464.

15 I. García-Orozco, R. Quijada, K. Vera and M. Valderrama, *J. Mol. Catal. A: Chem.*, 2006, **260**, 70.

16 A. J. L. Pombeiro, M. F. C. Guedes da Silva and M. A. N. D. A. Lemos, *Coord. Chem. Rev.*, 2001, **219**, 53.

17 (*a*) *Bruker, APEX2 & SAINT*, AXS Inc., Madison, WI, 2004; (*b*) G. M. Sheldrick, *Acta Crystallogr., Sect. A: Fundam. Crystallogr.*, 2008, **A64**, 112; (*c*) L. J. Farrugia, *J. Appl. Crystallogr.*, 1999, **32**, 837.

18 (*a*) M. K. Saha and I. Bernal, *Inorg. Chem. Commun.*, 2005, **8**, 871; (*b*) M. Prabhakar, P. S. Zacharias and S. K. Das, *Inorg. Chem. Commun.*, 2006, **9**, 899; (*c*) P. S. Lakshminarayanan, E. Suresh and P. Ghosh, *Angew. Chem., Int. Ed.*, 2006, **45**, 3807; (*d*) A. K. Ghosh, D. Ghoshal, J. Ribas, G. Mostafa and N. R. Chaudhuri, *Cryst. Growth Des.*, 2006, **6**, 36; (*e*) D. L. Reger, R. F. Semeniuc, C. Pettinari, F. Luna-Giles and M. D. Smith, *Cryst. Growth Des.*, 2006, **6**, 1068; (*f*) M. S. Deshpande, A. S. Kumbhar, V. G. Puranik and K. Selvaraj, *Cryst. Growth Des.*, 2006, **6**, 743.

19 L. Infantes, J. Chisholm and S. Motherwell, *CrystEngComm*, 2003, **5**, 480.

20 R. Ludwig, *Angew. Chem., Int. Ed.*, 2001, **40**, 1808.

21 (*a*) M. Mascal, L. Infantes and J. Chisholm, *Angew. Chem., Int. Ed.*, 2006, **45**, 32; (*b*) L. Infantes and S. Motherwell, *Cryst EngComm*, 2002, **4**, 454; (*c*) L. Infantes, J. Chisholm and S. Motherwell, *CrystEngComm*, 2003, **5**, 480; (*d*) S. Supriya and S. K. Das, *Clust. J. Sci.*, 2003, **14**, 337.

22 (*a*) Y. Y. Karabach, A. M. Kirillov, M. F. C. Guedes da Silva, M. N. Kopylovich and A. J. L. Pombeiro, *Cryst. Growth Des.*, 2006, **6**, 2200; (*b*) M. V. Kirillova, A. M. Kirillov, M. F. C. Guedes da Silva, M. N. Kopylovich, J. J. R. Fraústo da Silva and A. J. L. Pombeiro, *Inorg. Chim. Acta*, 2007, **360**, 506; (*c*) R. R. Fernandes, A. M. Kirillov, M. F. C. Guedes da Silva, Z. Ma, J. A. L. Silva, J. J. R. Fraústo da Silva and A. J. L. Pombeiro, *Cryst. Growth Des.*, 2008, **8**, 782–785.

23 L. D. Field, B. A. Messerle, L. P. Soler, T. W. Hambley and P. Turner, *J. Organomet. Chem.*, 2002, **655**, 146.

24 C.-W. Yu, K. K. W. Li, S.-K. Pang, S. C. F. Au-Yeung and Y.-P. Ho, *Bioorg. Med. Chem. Lett.*, 2006, **16**, 1686.

25 L. T. Vassilev, B. T. Vu, B. Graves, D. Carvajal, F. Podlaski, Z. Filipovic, N. Kong, U. Kammlott, C. Lukacs, C. Klein, N. A. Fotouhi and E. A. Liu, *Science*, 2004, **303**, 844.

26 N. Graf and S. J. Lippard, *Adv. Drug Delivery Rev.*, 2012, **64**, 993.

27 X. Zhang, J. Chen, B. Davis and F. Kiechle, *Arch. Pathol. Lab. Med.*, 1999, **123**, 921.

28 G. Zuber, J. C. Quada Jr. and S. M. Hecht, *J. Am. Chem. Soc.*, 1998, **120**, 9368.

29 F. R. Keene, J. A. Smith and J. G. Collins, *Coord. Chem. Rev.*, 2009, **253**, 2021.

30 L. J. K. Boerner and J. M. Zaleski, *Curr. Opin. Chem. Biol.*, 2005, **9**, 135.

31 (*a*) S. Ramakrishnan, E. Suresh, A. Riyasdeen, M. A. Akbarshad and M. Palaniandavar, *Dalton Trans.*, 2011, **40**, 3245; (*b*) S. Leonard, P. M. Gannett, Y. Rojanasakul, D. Schwegler-Berry, V. Castranova, V. Vallyathan and X. Shi, *J. Inorg. Biochem.*, 1998, **70**, 239.
32 B. Ward, A. Skorobogaty and J. C. Dabrowiak, *Biochemistry*, 1986, **25**, 6875.
33 R. J. Fiel, *J. Biomol. Struct. Dyn.*, 1989, **6**, 1259.
34 S. Yellappa, J. Seetharamappa, L. M. Rogers, R. Chitta, R. P. Singhal and F. D'Souza, *Bioconjugate Chem.*, 2006, **17**, 1418.
35 P.-Y. Liu, N. Jiang, J. Zhang, X. Wei, H.-H. Lin and X.-Q. Yu, *Chem. Biodiversity*, 2006, **3**, 958.
36 Y. Wang and B. Van Ness, *Nucleic Acids Res.*, 1989, **17**, 6915.
37 A. R. Morgan, R. L. Cone and T. M. Elgert, *Nucleic Acids Res.*, 1976, **3**, 1139.
38 (*a*) D. R. Eaton and A. O'Reilly, *Inorg. Chem.*, 1987, **26**, 4185; (*b*) Y. Ishii, S. Sakaguchi and T. Iwahama, *Adv. Synth. Catal.*, 2001, **343**, 393; (*c*) H. Arora, C. Philouze, O. Jarjayes and F. Thomas, *Dalton Trans.*, 2010, **39**, 10088.
39 R. Colognato, A. Bonelli, J. Ponti, M. Farina, E. Bergamaschi, E. Sabbioni and L. Migliore, *Mutagenesis*, 2008, **23**, 377.
40 E. L. Baldwin, J. A. Byl and N. Osheroff, *Biochemistry*, 2004, **43**, 728.
41 IARC Working Group on the Evaluation of Carcinogenic Risks to Humans, *IARC Monographs on the Evaluation of Carcinogenic Risks to Humans*, 2006, vol. 86, p. 35.
42 V. A. Kawade, A. A. Kumbhar, A. S. Kumbhar, C. Nather, A. Erxleben, U. B. Sonawaned and R. R. Joshid, *Dalton Trans.*, 2011, **40**, 639.
43 S. I. Kirin, C. M. Happel, S. Hrubanova, T. Weyhermüller, C. Klein and N. Metzler-Nolte, *Dalton Trans.*, 2004, 1201.
44 (*a*) P. M. Reis, J. A. L. Silva, J. J. R. F. Silva and A. J. L. Pombeiro, *Chem. Commun.*, 2000, 1845; (*b*) M. V. Kirillova, M. L. Kuznetsov, P. M. Reis, J. A. L. Silva, J. J. R. Fraústo da Silva and A. J. L. Pombeiro, *J. Am. Chem. Soc.*, 2007, **129**, 10531; (*c*) M. V. Kirillova, M. L. Kuznetsov, J. A. L. Silva, M. F. C. Guedes da Silva, J. J. R. Fraústo da Silva and A. J. L. Pombeiro, *Chem.–Eur. J.*, 2008, **14**, 182; (*d*) R. R. Fernandes, M. V. Kirillova, J. A. L. Silva, J. J. R. Fraústo da Silva and A. J. L. Pombeiro, *Appl. Catal., A*, 2009, **353**, 107; (*e*) M. V. Kirillova, A. M. Kirillov and A. J. L. Pombeiro, *Adv. Synth. Catal.*, 2009, **351**, 2936; (*f*) M. V. Kirillova, A. M. Kirillov, M. L. Kuznetsov, J. A. L. Silva, J. J. R. Fraústo da Silva and A. J. L. Pombeiro, *Chem. Commun.*, 2009, 2353; (*g*) A. M. Kirillov, J. A. S. Coelho, M. V. Kirillova, M. F. C. Guedes da Silva, D. S. Nesterov, K. R. Gruenwald, M. Haukka and A. J. L. Pombeiro, *Inorg. Chem.*, 2010, **49**, 6390; (*h*) M. V. Kirillova, A. M. Kirillov and A. J. L. Pombeiro, *Chem.–Eur. J.*, 2010, **16**, 9485; (*i*) M. V. Kirillova, A. M. Kirillov and A. J. L. Pombeiro, *Appl. Catal., A.*, 2011, **401**, 106.